Proceedings of the 6th ITB International Graduate School Conference
Multidisciplinary Collaboration for Sustainable Energy: Science, Technology, Policy, and Society

Design of a Computational Tool for Organic Rankine Cycle Performance Estimation Based on Geothermal Field Data

Singgih Imam Kurniawan[1,4,*], Ali Ashat[2], & Prihadi Setyo Darmanto[3]
[1] Geothermal Engineering Master's Program - Faculty of Mining and Petroleum Engineering, Institut Teknologi Bandung, Jl. Ganesha 10, Bandung 40132, Indonesia
[2] Faculty of Mining and Petroleum Engineering, Institut Teknologi Bandung, Jl. Ganesha 10, Bandung 40132, Indonesia
[3] Faculty of Mechanical and Aerospace Engineering, Institut Teknologi Bandung, Jl. Ganesha 10, Bandung 40132, Indonesia
[4] PT PLN (Persero), Jalan Trunojoyo Blok M-1 No.135, Jakarta, Indonesia
*email: singgih.imam.kurniawan@gmail.com

Abstract.

This study evaluates the thermodynamic feasibility of additional power generation from separated brine at a high-temperature geothermal plant in Indonesia, referred to as the "XYZ geothermal plant" to maintain site confidentiality. The plant operates with a single-phase liquid-dominated reservoir, with temperatures ranging from 250 °C to 270 °C and a brine reinjection temperature of approximately 170 °C at a flow rate of 1400 tons per hour.

To ensure safe reinjection conditions, the Silica Scaling Index (SSI) was applied to determine the minimum allowable brine temperature. A finite difference-based Python simulation tool was developed to model heat transfer in the ORC system and assess performance across different working fluids and operating pressures. The results show that n-pentane achieves the best performance, producing a net power output of 5596 kW and a thermal efficiency of 17.21% at an optimal pressure of 1.80 MPa. Isopentane follows closely, while R-1233zd(E) performs less favorably due to pressure constraints.

Model validation against manual calculations resulted in deviations below 0.6%, confirming the simulation's accuracy. This tool provides a fast and reliable method for evaluating ORC performance and supports practical decision-making for geothermal plant operators. It is intended to assist utilities such as PLN in optimizing geothermal resource utilization.

Keywords: *organic rankine cycle, brine, silica scaling index, simulation tool.*

1 Introduction

In this study, process data were obtained from a geothermal plant referred to as the "XYZ geothermal plant," a placeholder used to maintain the confidentiality

of the actual facility name, in accordance with the industrial partner's request. The plant utilizes a single-phase liquid-dominated geothermal resource, with reservoir temperatures ranging from 250°C to 270°C. The brine is reinjected into the reservoir at approximately 170°C, with a total flow rate of about 1400 tons per hour from the existing separators [1].

The Organic Rankine Cycle (ORC) offers a solution to improve energy utilization efficiency in geothermal power plants by harnessing waste heat that is no longer usable in the main steam cycle. This technology employs organic working fluids with low boiling points, enabling the conversion of thermal energy at temperatures that are no longer economical for conventional steam cycles. One of the main challenges in the development of organic Rankine cycle (ORC) systems lies in the selection of a suitable working fluid and the appropriate cycle configuration. As noted by Saleh *et al.* [2], the process must achieve high thermal efficiency and enable optimal utilization of the available heat source. Furthermore, the working fluid should meet safety standards, be environmentally benign, and contribute to minimizing the overall cost of the power plant.

Dry-type working fluids are employed in this study due to their favorable thermodynamic behavior—specifically, a positively sloped saturated vapor line in the temperature–entropy (T–s) diagram. This characteristic helps avoid wet vapor formation at the turbine outlet, which could lead to blade erosion from liquid droplet impingement. Moreover, dry fluids do not require superheating to maintain vapor dryness, simplifying system design and improving efficiency in low-temperature geothermal applications.

Given the geothermal brine temperature of approximately 170 °C, the selected fluids have critical temperatures moderately close to the heat source. This allows evaporation to occur under subcritical conditions, mitigates inefficiencies near the critical point, and ensures sufficient vapor density across both high- and low-pressure sides of the cycle. Although some studies suggest that fluids with higher critical temperatures may improve thermal efficiency, they often result in lower vapor densities and increased system cost. As highlighted by Quoilin et al. [3], optimizing the match between heat source temperature and the fluid's critical point is essential to balance thermal and economic performance in ORC systems.

A thermodynamic analysis was conducted to evaluate the performance of the Organic Rankine Cycle (ORC) system under pinch point temperature constraints. A finite difference-based heat exchanger model was developed to simulate temperature profiles and determine pinch point temperature differences under varying turbine inlet pressures. Thermodynamic outputs were analyzed across several pinch point scenarios to identify the optimal trade-off between efficiency and heat source utilization. All simulations were conducted using REFPROP 10.0

integrated into Microsoft Excel. Prior to simulation, a silica scaling analysis was performed to define safe reinjection temperatures. The results offer a comprehensive framework for evaluating ORC configurations under geothermal and mineral scaling constraints.

2 Materials and methods

2.1 Materials

The brine data from the XYZ geothermal field, used as the heat source in this study, are summarized as follows:

Table 1 Summary of brine parameter [1]

Parameter	Value	Unit	Descriptions
T brine	170	^{0}C	Brine inlet temperature
P brine	7.5	bar	Brine pressure
m brine	388.89	kg/s	Combine flow from 2 separators
Cl^-	705	ppm	Cloride content
Si	615	ppm	Silica content
Average ambient temp	23	^{0}C	Inlet air cooler temp

Considering the selection criteria that include working fluids with critical temperatures approximately near 170°C—both slightly above and below—as presented by Ata et al. [4] and other supporting references, several organic fluids have been identified as potential candidates for subcritical ORC systems. These are listed in Table 2 .

Table 2 Thermophysical and safety-environmental properties of fluids for low-temperature ORC [4] .

Fluid	R601	R601a	R123	R245fa	R-1233zd(E)
Type	Dry	Dry	Isentropic	Dry	Dry
Molecular mass (g/mol)	72.15	72.15	152.93	134.05[5]	130.5 [5]
Normal Boiling Points (^{o}C)	36.1	27.8	27.8	15.04[5]	18.3 [5]
Critical Temperature (^{o}C)	196.6	187.2	183.7	153.86[5]	166.5 [5]
Critical Pressure (MPa)	3.37	3.38	3.66	3.65[5]	3.62 [5]
ASHRAE 34 safety group	A3	A3	B1	B1[6]	A1[6]
ODP	0	0	0.2[7]	0[8]	<0.0004[8]
GWP	20	20	77	1030 [8]	3.4 [8]

Fluid	R601	R601a	R123	R245fa	R-1233zd(E)

Environmental considerations are critical in the selection of organic working fluids for Organic Rankine Cycle (ORC) systems. Two principal environmental metrics are the Ozone Depletion Potential (ODP) and the Global Warming Potential (GWP). Fluids with nonzero ODP are recognized contributors to stratospheric ozone layer degradation and are regulated under international frameworks such as the Montreal Protocol. This regulation encompasses Class I substances (e.g., chlorofluorocarbons with ODP ≥ 0.2) and Class II substances (e.g., hydrochlorofluorocarbons with ODP < 0.2), all of which are subject to a scheduled phase-out irrespective of their specific ODP values [9]. Additionally, the Kigali Amendment mandates the progressive reduction of high-GWP substances, particularly targeting those with GWP values exceeding 150, which are increasingly restricted in many jurisdictions [10]. Consequently, working fluids with ODP = 0 and GWP < 150 are generally preferred for environmentally sustainable ORC applications.

Hydrocarbons such as isopentane (R601a) and n-pentane (R601), as well as hydrofluoroolefins (HFOs) such as R-1233zd(E), fulfill these environmental criteria and are therefore considered promising candidates for low- and medium-temperature ORC systems. Beyond environmental performance, commercial availability and proven practical application in ORC systems are also essential selection criteria. R601 and R601a are commercially supplied by manufacturers such as Haltermann Carless [11], while R-123 is produced by Chemours [12]. Furthermore, fluids like R-245fa and R-1233zd(E) are manufactured by Honeywell and are widely adopted in ORC systems designed for low-ODP operation [13].

ORC systems utilizing R601 and R601a have been successfully deployed at commercial scale by major industry players such as Ormat Technologies Inc. [3]. In contrast, R-123 is infrequently employed in large-scale ORC installations and is more commonly found in academic research or pilot-scale systems, largely due to its nonzero ODP and corresponding regulatory constraints.

Based on the combined criteria of critical temperature range, environmental acceptability (in terms of ODP and GWP), commercial availability, and safety classification as defined by ASHRAE Standard 34, the working fluids selected for evaluation in this study are n-pentane (R601), isopentane (R601a), and R-1233zd(E). Although R-245fa exhibits favorable thermodynamic performance and negligible ozone depletion potential (ODP ≈ 0), its classification as a B1 refrigerant under ASHRAE Standard 34—indicating higher toxicity despite low

flammability—raises safety concerns, particularly in contexts involving occupational exposure or the risk of fluid leakage. In addition, its global warming potential (GWP) exceeds 150, which does not align with emerging regulatory thresholds and sustainability targets for low-GWP working fluids. These factors collectively reduce the suitability of R-245fa for environmentally responsible ORC applications. The assumed operational design parameters are as follows:

Table 3 Assumption design parameter

Parameter	Value	Unit
Pinch point temperature difference target	5	^{0}C
Turbine isentropic efficiency	90	%
Pump efficiency	75	%
Condenser Temperature	37	^{0}C
Air cooler inlet temperature	30	^{0}C
Air cooler outlet temperature	50	^{0}C

2.2 Method

The thermodynamic evaluation of the Organic Rankine Cycle (ORC) system is conducted based on the fundamental principles of the Rankine cycle, as depicted in the schematic diagram Figure 1.

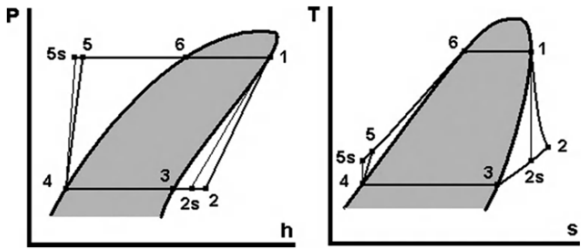

Figure 1 P–H and T–S Diagrams for Binary Power Plants [14]

The energy performance of each system component is evaluated based on the first law of thermodynamics [14]. The work produced by the turbine is calculated using its isentropic efficiency (1). The heat rejected in the condenser is determined from the enthalpy drop of the working fluid (2). Pump work is calculated by considering the isentropic compression process and pump efficiency (3) and (4). Finally, the heat input to the evaporator is obtained from the enthalpy rise of the working fluid (5). The corresponding equations are given below:

$$W_t = \dot{m}_{wf}(h1 - h2) = \dot{m}_{wf}\eta_t(h1 - h2s) \quad (1)$$

$$Q_c = \dot{m}_{wf}(h2 - h3) \tag{2}$$

$$W_{ps} = \dot{m}_{wf}(h5s - h4) = \dot{m}_{wf} v4(P5s - P4) \tag{3}$$

$$W_p = \dot{m}_{wf}(h5 - h4) = \dot{m}_{wf}(h5s - h4)/\eta_p \tag{4}$$

$$Q_{in} = \dot{m}_{wf}(h1 - h5) \tag{5}$$

The mass flow rate of the working fluid is calculated based on the energy balance in the preheater and condenser sections, as expressed by the following equations:

$$\dot{m}_b C_{p,b}(TA - TC) = \dot{m}_{wf}(h1 - h5) \tag{6}$$

The fan power is estimated based on the air mass flow rate during condensation (7) and the fan power is obtained by multiplying the air mass flow rate by a specific consumption of 0.15 kW per kg/s of air (8), as suggested by Toffolo et al. (2014) [15], calculated as:

$$Q_c = m_{air} C_{p,air}(T_{out,air} - T_{in,air}) \tag{7}$$

$$W_{fan} = 0.15\, m_{air} \tag{8}$$

The net power output (9) and thermal efficiency (10) is calculated by neglecting electrical conversion efficiency. The analysis is based on fixed thermodynamic conditions of the available geothermal fluid. The internal power consumption components are defined as follows:

$$W_{net} = W_t - W_p - W_{fan} \tag{9}$$

$$\eta_{th} = \frac{W_{net}}{Q_{in}} \tag{10}$$

In this study, it is assumed that the working fluid undergoes phase change (evaporation) at the pinch point temperature difference within the heat exchanger. Accordingly, pinch analysis serves as a constraint that defines the maximum evaporation temperature achievable by the working fluid. To determine this upper limit, a finite difference method is applied along the heat exchanger domain. This approach is adapted— with slight modifications— from the discretized model developed by Denkenberger et al. [16] assuming steady-state flow and axial discretization of parallel channels to assess flow maldistribution effects, which originally used the energy balance:

$$0 = \dot{q}_{cov,c,i,j} - \dot{q}_{cov,c,o,j} + \dot{q}_{tran,c,,j} \tag{11}$$

In contrast, the present work employs a simplified energy-based formulation:

$$\dot{Q}_{brine} = \dot{m}_b C_{p,b}(T_{i+1} - T_i) \tag{12}$$

$$\dot{Q}_{wf} = \dot{m}_{wf}(h_{i+1} - h_i) \tag{13}$$

By equating the segmental heat transfer between hot and cold sides ($\dot{Q}_{brine} = \dot{Q}_{wf}$), the enthalpy change Δh of the working fluid is estimated and subsequently used to evaluate its corresponding temperature through thermophysical property data. The cumulative heat transfer (Q) for both streams is plotted against temperature, resulting in composite T–Q curves. The point of minimum temperature difference between the curves identifies the pinch point.

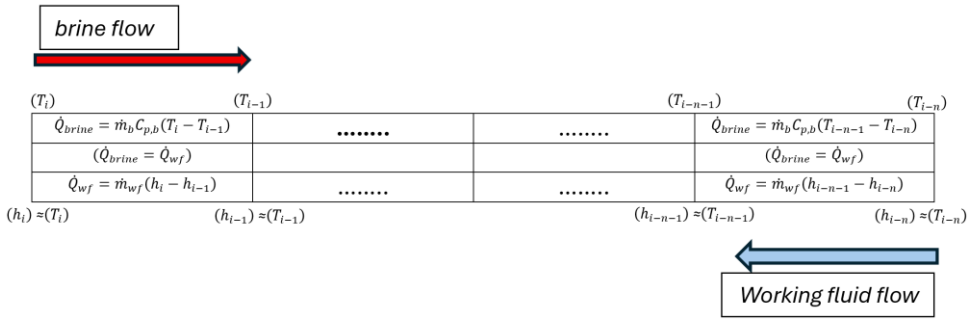

Figure 2 Finite Difference Segmental Heat Transfer Model for Counter-Flow Heat Exchanger

2.2.1 Scaling Analysis

Silica precipitation occurring at the surface (where temperatures are lower than reservoir conditions) is controlled by equilibrium with amorphous silica, which is more soluble than quartz. The relationship between amorphous silica solubility and temperature is described by the Fournier and Rowe equation:

$$\log C = 4.52 - (731/T) \tag{14}$$

where C is the silica concentration in mg/kg, and T is the temperature in kelvin. Similar to quartz, the solubility of amorphous silica is also affected by salinity. The influence of salinity on silica solubility is described by the Setchenow equation [14]:

$$S(T,m)=C_{(T,m=0)}\times 10^{-mD(t)} \tag{15}$$

where $S_{(T,m)}$ is the corrected solubility of silica in mg/kg at temperature T (in kelvin) and salinity m (in molal). The parameter D(t) is defined by Chen and Marshall [14] as:

$$\text{Log } D(t) = -1.0596 - 0.001573\ t \tag{16}$$

where t is the temperature in degrees Celsius. When SSI > 1, the fluid is in a supersaturated state and silica precipitation is likely to occur.

2.2.2 Calculation Method and Software Implementation

The initial thermodynamic calculations were performed using Microsoft Excel integrated with REFPROP 10.0, a software developed by NIST for calculating thermophysical properties. Following this, a computational model was developed using the Python programming language. The development of the Python code, including the integration of the ctREFPROP library, was assisted by ChatGPT, a Generative AI tool based on large language models, under direct human supervision. ChatGPT was also utilized to refine the grammar and enhance the clarity of the English-language content. All modeling logic, implementation, and validation were carried out and verified independently by the authors.

Thermophysical properties of the working fluids—such as isopentane, pentane, and R-1233zd(E)—were obtained using ctREFPROP, which interfaces with REFPROP 10.0. The modeled subcritical Organic Rankine Cycle (ORC) consists of six state points. The simulation calculates turbine and pump work, working fluid mass flow rate (based on heat extracted from brine), and net power output. Validation of the Python-based results was performed through comparison with Excel-based manual calculations.

2.2.3 Limitations of the Model

The ORC simulation developed in this work relies on a steady-state, single-pressure cycle model implemented using REFPROP for thermophysical property calculations. Several simplifications and assumptions introduce limitations to the analysis. First, the model neglects electrical conversion efficiency and assumes ideal heat transfer within the preheater and evaporator without accounting for pressure drops, heat losses to the environment, or flow maldistribution. The mass flow rate of the working fluid is derived from an energy balance using fixed brine inlet and outlet conditions, without iterative coupling to a detailed heat exchanger model. Fan power is estimated based on empirical specific consumption, while the condenser is treated using simplified air-side energy balance. Additionally, the optimization of the evaporator pressure to match a target pinch point temperature difference is performed under the assumption of constant specific heat and segmented linear heat transfer. These assumptions, while useful for preliminary analysis, may limit the accuracy of results when applied to real operating conditions or detailed system design.

3 Results and Discussion

3.1 Results

The first step of this study involved evaluating the silica solubility potential using the Silica Scaling Index (SSI) method. This step aimed at determining the minimum allowable brine reinjection temperature that would prevent silica precipitation within the injection pipeline. The results of the silica scaling index calculation indicate that the SSI value exceeds 1 when the reinjection brine temperature falls below 150 °C, as shown in Figure (3).

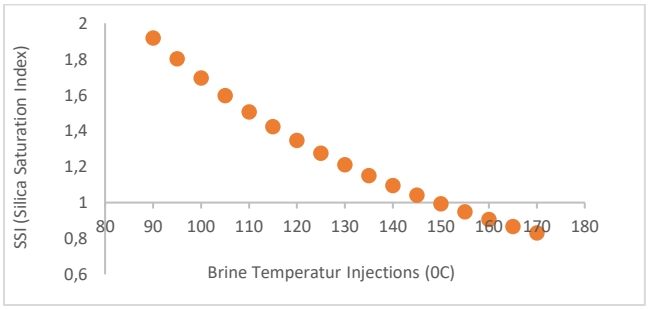

Figure 3 Silica Scaling Index Calculation

After determining the injection temperature limit of the brine to prevent silica scaling, a thermodynamic analysis was carried out using the input parameters previously described in Section (2). The initial calculations were performed using Microsoft Excel for the three selected working fluids. Subsequently, variations in evaporator pressure were applied to evaluate the resulting pinch point temperature differences corresponding to each pressure increment, as shown in Figure 4a-c.

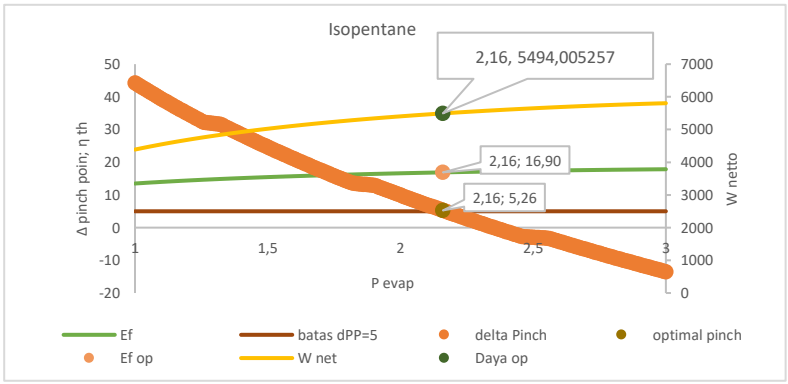

a. Isopentane

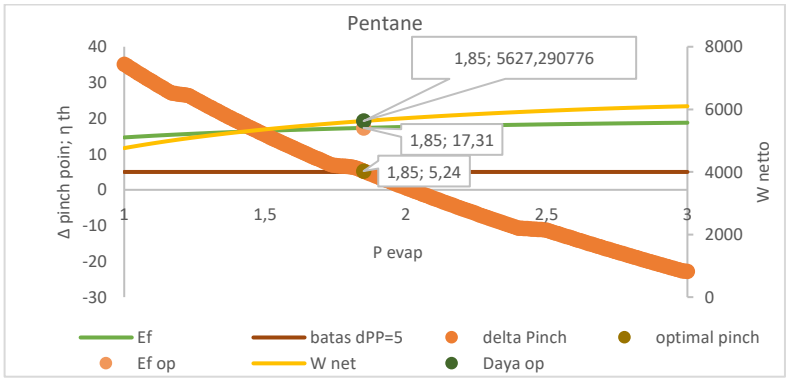

b. Pentane

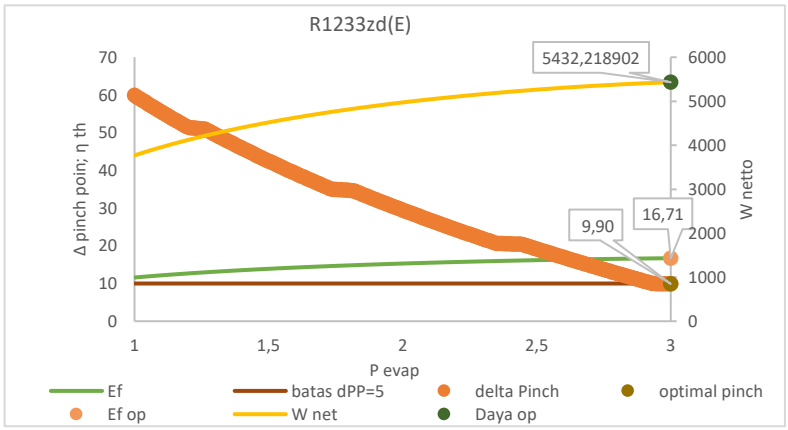

c. R1233zd(E)

Figure 4 Effect of evaporator pressure on pinch point temperature difference, net power output, and thermal efficiency for n-pentane

The results indicate that a pinch point temperature difference of 5 °C was achieved at 2.16 MPa for isopentane and at 1.85 MPa for n-pentane, while this condition could not be achieved for R1233zd(E). The corresponding net power output and thermal efficiency at a 5 °C pinch point were 5495 kW (16.9%) for isopentane and 5627 kW (17.3%) for n-pentane. For R1233zd(E), even at an evaporator pressure of 3 MPa, a 5 °C pinch point was not attainable. It is important to note that R-1233zd(E) could not reach a 5°C pinch point temperature within the pressure constraint of 3.0 MPa, which was imposed based on safety and equipment design limitations. As observed by Quoilin et al. [3], pressures in Organic Rankine Cycle systems typically do not exceed 30 bar, since higher pressures tend to increase system complexity and capital cost. Instead, a pinch point of 9.9 °C was observed at this pressure, with a net power output of 5432 kW and a thermal efficiency of 16.71%.

After the initial manual calculations, a computational model was developed in Python to simulate the heat exchange process under varying evaporator pressures. The simulation results are presented in Figures 5–7 and Table 4. A finite difference segmental approach was used to model the stepwise heat transfer within the heat exchanger. The T–Q diagrams illustrate how the pinch point temperature and its position shift with changes in evaporator pressure. The optimal pressure for each working fluid was identified through iterative simulation to achieve a target pinch point temperature, highlighting the sensitivity of heat exchanger performance to pressure variations

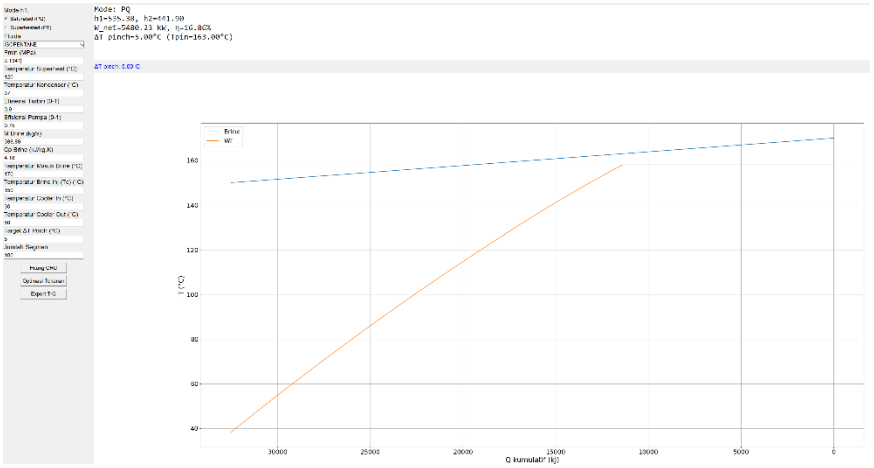

Figure 5 T–Q diagrams of isopentane at Δ pinch poin 5 °C.

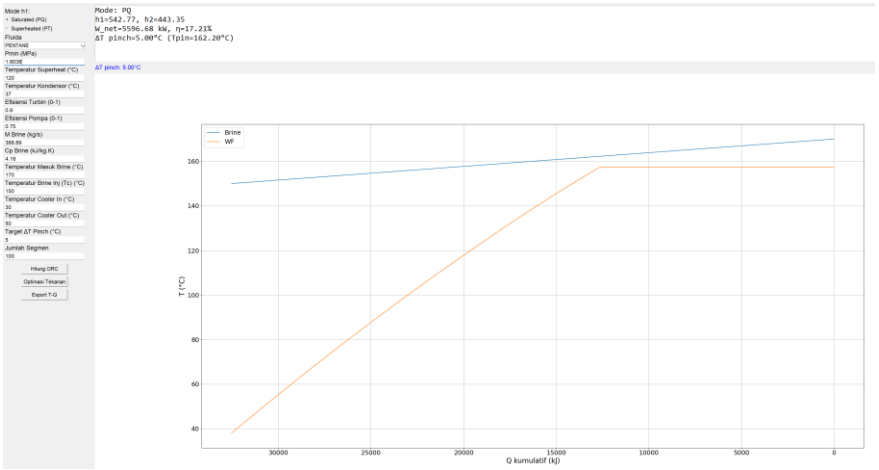

Figure 6 T–Q diagrams of pentane at Δ pinch poin 5 °C

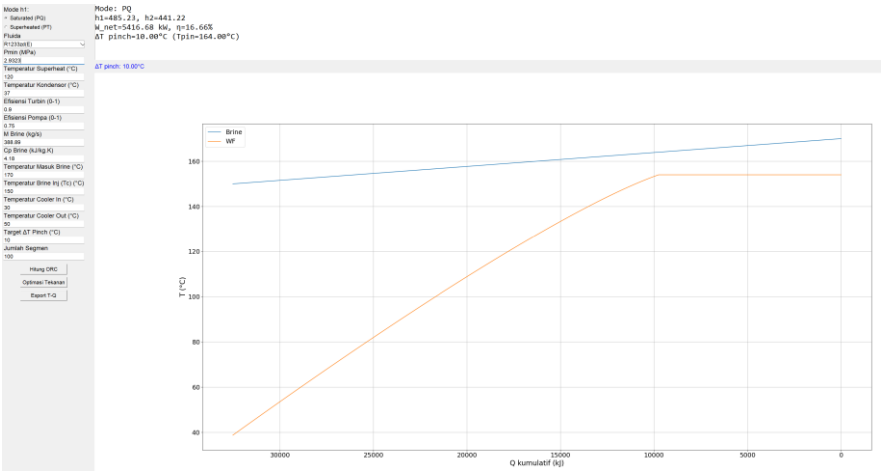

Figure 7 T–Q diagrams of R1233zd(E) at Δ pinch poin 5 °C

A performance comparison was carried out for three working fluids—isopentane, n-pentane, and R-1233zd(E)—under a pinch point temperature difference scenario of 5 °C. For isopentane and n-pentane, the 5 °C pinch point was achieved by adjusting the evaporator pressure accordingly. However, for R-1233zd(E), this condition could not be attained within the 3 MPa pressure constraint. The analysis focused on three key performance indicators: optimal turbine inlet pressure, net power output, and thermal efficiency. The results are summarized in Table 4.

Table 4 ORC Performance of Selected Working Fluids under Different Pinch Point Temperature Constraints.

	Isopentane (a)	**Pentane (b)**	**R-1233zd(E) (c)**
Pinch Point Temp (°C)	5	5	10
Optimal Turbine Inlet Pressure (MPa)	2.13	1.80	2.93
Net Power Output (kW)	5480	5596	5416
Thermal Efficiency (%)	16.86	17.21	16.66

3.2 Discussion

A side-by-side comparison shows excellent agreement between the manual Excel calculations and the Python-based finite-difference simulation:

Table 5 Comparative Accuracy of Manual Excel Calculations vs. Python Simulation

Parameter	**Isopentane**			**n-Pentane**			**R-1233zd€**		
	Manual (Excel)	**Simulation (Python)**	**%Error (abs)**	**Manual (Excel)**	**Simulation (Python)**	**%Error (abs)**	**Manual (Excel)**	**Simulation (Python)**	**%Error (abs)**
Net power, kW	**5495**	**5480**	**0.273**	**5627**	**5596**	**0.551**	**5432**	**5416**	**0.295**

Parameter	Isopentane			n-Pentane			R-1233zd€		
	Manual (Excel)	Simulation (Python)	%Error (abs)	Manual (Excel)	Simulation (Python)	%Error (abs)	Manual (Excel)	Simulation (Python)	%Error (abs)
Thermal efficiency, %	16.9	16.86	0.237	17.3	17.21	0.52	16.71	16.66	0.299
Opt. evaporator P, MPa	2.16	2.13	1.38	1.85	1.8	2.70	3	2.93	2.33

Net power output differs by < 0.6 % for all fluids, with the largest deviation observed for n-pentane. Thermal efficiency discrepancies remain below 0.55 %, confirming that the iterative pinch-point routine is consistently captured in both approaches. Optimal evaporator pressure predictions vary by ≤ 2.7 %, a margin acceptable for preliminary design. These small errors validate the Python model as a reliable replacement for spreadsheet-based calculations, offering automated convergence and easier sensitivity analyses while maintaining quantitative fidelity.

4 Conclusions

The simulation results indicate that both isopentane and n-pentane are effective working fluids under a 5 °C pinch point temperature difference. Among the three fluids evaluated, n-pentane exhibits the best overall thermodynamic performance, achieving a net power output of 5596 kW and a thermal efficiency of 17.21% at an optimal evaporator pressure of 1.80 MPa. This moderate pressure offers operational advantages such as reduced mechanical stress, lower compressor workload, and potentially lower equipment costs.

Isopentane, while slightly less efficient, also shows strong performance with a net power output of 5480 kW, a thermal efficiency of 16.86%, and a higher optimal pressure of 2.13 MPa. The higher pressure requirement may result in increased pump energy consumption and more demanding material specifications.

R-1233zd(E), evaluated at a 10 °C pinch point due to a pressure constraint of 3 MPa, showed the least favorable results, with a net power output of 5416 kW, thermal efficiency of 16.66%, and the highest evaporator pressure among the fluids (2.93 MPa). These characteristics limit its suitability for systems with strict pressure boundaries, despite its environmentally friendly profile.

To assess the reliability of the simulation, a comparative analysis with manual Excel-based calculations was performed. The deviations in net power, efficiency, and optimal pressure were found to be less than 0.6%, confirming the accuracy of the finite difference model. This validates the simulation as a robust tool for parametric evaluation and working fluid optimization in ORC system design.

While this study provides a detailed thermodynamic assessment, further research is recommended to include an economic analysis considering component costs, equipment constraints, and the potential for silica scaling. The feasibility of implementing silica treatment should be compared against the projected gains in power output, allowing for a more comprehensive working fluid selection based on both technical and economic criteria.

References

[1] PLN, "Feasibility Study of a Binary Geothermal Power Plant at the XYZ Site," 2024, *unpublished manuscript*.

[2] B. Saleh, G. Koglbauer, M. Wendland, and J. Fischer, "Working fluids for low-temperature organic Rankine cycles," *Energy*, vol. 32, no. 7, pp. 1210–1221, 2007, doi: 10.1016/j.energy.2006.07.001.

[3] S. Quoilin, M. Van Den Broek, S. Declaye, P. Dewallef, and V. Lemort, "Techno-economic survey of organic rankine cycle (ORC) systems," 2013. doi: 10.1016/j.rser.2013.01.028.

[4] S. Ata, A. KAHRAMAN, and R. ŞAHİN, "Determination of Optimum Pinch Point Temperature Difference Depending on Heat Source Temperature and Organic Fluid with Genetic Algorithm," *Academic Platform Journal of Engineering and Smart Systems*, vol. 10, no. 1, pp. 19–29, Jan. 2022, doi: 10.21541/apjess.1060748.

[5] M. L. H. and M. O. M. E. W. Lemmon, "NIST Reference Fluid Thermodynamic and Transport Properties—REFPROP, Version 10.0," 2018, *National Institute of Standards and Technology, Boulder, CO*: 10.

[6] ANSI/ASHRAE Standard 34-2019, "Designation and Safety Classification of Refrigerants," 2019. [Online]. Available: www.ashrae.org

[7] Ozone Secretariat, *Handbook for the Montreal Protocol on Substances that Deplete the Ozone Layer*, Fourteenth edition. Nairobi, Kenya: United Nations Environment Programme, 2020.

[8] U.S. Environmental Protection Agency, "Substitutes in Industrial Process Air Conditioning," Significant New Alternatives Policy (SNAP) Program," https://www.epa.gov/snap/substitutes-industrial-process-air-conditioning. [Accessed: 31-May-2025].

[9] U.S. Environmental Protection Agency, "Phaseout of Class II Ozone-Depleting Substances," https://www.epa.gov/ods-phaseout/phaseout-class-ii-ozone-depleting-substances.

[10] California Energy Codes and Standards, "Refrigerants and Climate Change," 2022. Accessed: Jun. 01, 2025. [Online]. Available: http://gettingtozeroforum.org

[11] Haltermann Carless, "High-Purity Hydrocarbons," https://www.haltermann-carless.com.
[12] Chemours Company, "Freon™ 123 Refrigerant," https://www.chemours.com.
[13] Honeywell, "Honeywell-Refrigerants-Roadmap_EN_2018," https://www.honeywell-refrigerants.com/europe/wp-content/uploads/2016/04/Honeywell-Refrigerants-Roadmap_EN_2018.pdf.
[14] P. D. Ronald DiPippo, *Geothermal Power Plants: Principles, Applications, Case Studies and Environmental Impact*, 3th ed. UK: Butterworth-Heinemann, 2012.
[15] A. Toffolo, A. Lazzaretto, G. Manente, and M. Paci, "A multi-criteria approach for the optimal selection of working fluid and design parameters in Organic Rankine Cycle systems," *Appl Energy*, vol. 121, pp. 219–232, May 2014, doi: 10.1016/j.apenergy.2014.01.089.
[16] D. C. Denkenberger, M. J. Brandemuehl, J. Zhai, and J. M. Pearce, "Finite Difference Heat Exchanger Model: Flow Maldistribution with Thermal Coupling," *Heat Transfer Engineering*, vol. 42, no. 11, pp. 889–903, 2021, doi: 10.1080/01457632.2020.1756060.